

# Remarkable Shape-Sustaining, Load-Bearing, and Self-Healing Properties Displayed by a Supramolecular Gel Derived from a Bis-pyridyl-bis-amide of L-Phenyl Alanine

Uttam Kumar Das,<sup>[a]</sup> Subhabrata Banerjee,<sup>[b]</sup> and Parthasarathi Dastidar\*<sup>[a]</sup>

**Abstract:** A series of bis-amides decorated with pyridyl and phenyl moieties derived from L-amino acids having an innocent side chain (L-alanine and L-phenyl alanine) were synthesized as potential low-molecular-weight gelators (LMWGs). Both protic and aprotic solvents were found to be gelled by most of the bis-amides with moderate to excellent gelation efficiency (minimum gelator concentration = 0.32–4.0 wt. %

and gel–sol dissociation temperature  $T_{\text{gel}} = 52\text{--}110^\circ\text{C}$ ). The gels were characterized by rheology, DSC, SEM, TEM, and temperature-variable  $^1\text{H NMR}$  measurements. pH-dependent gelation studies revealed that the pyridyl moiety

took part in gelation. Structure–property correlation was attempted using single-crystal X-ray and powder X-ray diffraction data. Remarkably, one of the bis-pyridyl bis-amide gelators, namely **3,3-Phe** (3-pyridyl bis-amide of L-phenylalanine) displayed outstanding shape-sustaining, load-bearing, and self-healing properties.

**Keywords:** gelators • load-bearing • self-healing • supramolecular gels • X-ray diffraction

## Introduction

Low-molecular-weight gelators (LMWGs) are small molecules ( $MW \leq 3000$ ) capable of immobilizing a large volume of solvent resulting in semi-solid viscoelastic materials called gels.<sup>[1]</sup> Various supramolecular interactions such as hydrogen bonding, halogen bonding, van der Waals forces, and  $\pi\text{--}\pi$  stacking are responsible for forming one-dimensional (1D) fibrous networks known as self-assembled fibrillar networks (SAFINs),<sup>[1b]</sup> in which the solvent molecules are immobilized, thus resulting in a gel. Due to the various potential applications of gels in oil recovery,<sup>[2]</sup> sensors,<sup>[3]</sup> conservation of art,<sup>[4]</sup> electro-optics/phonics,<sup>[5]</sup> cosmetics,<sup>[6]</sup> structure-directing agents,<sup>[7]</sup> catalysis,<sup>[8]</sup> drug delivery,<sup>[9]</sup> biomedical applications,<sup>[10]</sup> etc., the research activity in the field of supramolecular gels has been growing significantly in recent years. The gel matrix can be used for crystallization as well.<sup>[11]</sup> Recently, efforts have been undertaken in developing gels that

have remarkable self-standing or shape-sustaining, load-bearing, and self-healing properties.<sup>[12–14]</sup> These properties are expected to be useful in external coatings, architectural materials, artificial cartilage, drug-delivery systems, biosensors, etc.<sup>[15–22]</sup>

The structural diversity of known gelators—from simple organic salts<sup>[23]</sup> to bis-urea derivatives,<sup>[24]</sup> peptides,<sup>[25]</sup> carbohydrates,<sup>[26]</sup> anthracene derivatives,<sup>[27]</sup> surfactants,<sup>[28]</sup> phthalocyanines,<sup>[29]</sup> porphyrins,<sup>[30]</sup> cholesterol,<sup>[31]</sup> etc., and the lack of understanding of the gel-forming mechanism at the molecular level make it difficult to design new gelator molecules. Nevertheless, there have been few reports on the design of LMWGs. For example, Weiss et al. have designed aromatic-linker-steroid (ALS)-based gelators.<sup>[32]</sup> van Esch et al. have designed  $C_3$ -symmetric hydrogelators by balancing the hydrophobicity and the hydrophilicity of the gelling scaffold.<sup>[33]</sup> Our group, on the other hand, made significant contributions to designing LMWGs following a supramolecular synthon approach in the context of crystal engineering.<sup>[23]</sup> Recently, we demonstrated that the supramolecular synthon approach was indeed useful in developing gelators capable of displaying a slow release of pheromones,<sup>[34]</sup> reverse thermal gelation,<sup>[35]</sup> gel-sculpture, load-bearing, and self-healing properties,<sup>[36]</sup> and in vivo self-delivery of a drug.<sup>[37]</sup> In this report, we chose to explore well-studied supramolecular interactions involving an amide functionality to develop supramolecular gelators having an innocent L-amino acid backbone. The amide functional group, being one of the most studied supramolecular functionalities, is known to impart gelation through hydrogen bonding. While a secondary monoamide forms a 1D hydrogen bond network through  $\text{N–H}\cdots\text{O}$  interactions, a bis-amide generates a beta-sheet-

[a] Dr. U. K. Das, Dr. P. Dastidar  
Department of Organic Chemistry  
Indian Association for the Cultivation of Science (IACS)  
2A and 2B, Raja S. C. Mullick Road, Jadavpur, Kolkata-700032, West Bengal (India)  
Fax: (+91) 33-2473-2805  
E-mail: ocpd@iacs.res.in  
parthod123@rediffmail.com

[b] Dr. S. Banerjee  
Present address:  
National Institute of Advanced Industrial Science and Technology (AIST)  
AIST Central 5-2, 1-1-1 Higashi, Tsukuba, Ibaraki 305-8565 (Japan)

Supporting information for this article is available on the WWW under <http://dx.doi.org/10.1002/asia.201402053>.

like 1D hydrogen bond network. Both mono- and bis-amides are known to impart gelation.<sup>[38]</sup> In this work, we considered various bis-amides having terminal moieties like various positional isomers of pyridyl moieties, which can also take part in hydrogen bonding interactions; we also studied the corresponding phenyl derivatives to probe the role of pyridyl moieties in gelation (Figure 1). One such gelator (**3,3-Phe**) displayed remarkable shape-sustaining, load-bearing, and self-healing properties.

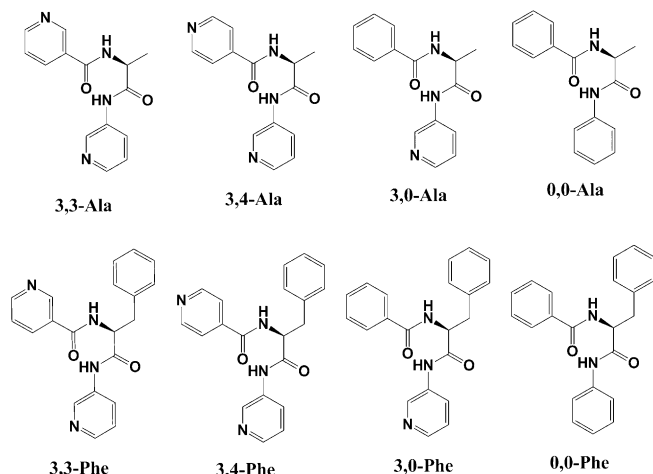


Figure 1. Various bis-amide derivatives of L-phenylalanine and L-alanine studied herein.

## Results and Discussion

### Syntheses

The bis-amides investigated (see Figure 1) were synthesized as follows: An N-Boc-L-amino acid was reacted with the corresponding amine by DCC coupling. After deprotecting the N-Boc group of the resultant mono-amide, it was react-

ed with the corresponding acid chloride to obtain the final bis-amide derivatives with an average overall yield of about 65 % (see the Experimental Section).

### Gelation Studies

The compounds were scanned for gelation tests in 15 selected polar and nonpolar solvents (Table 1). Gel formation was confirmed by tube inversion experiments. All the gels obtained were thermoreversible and stable for months at ambient temperature. While **3,3-Ala**, **0,0-Phe**, and **0,0-Ala** acted as a nongelator, hydrogelator, and ambidextrous gelator, respectively, the remaining compounds were found to be organogelators. The terminal moieties and amino acid side chain had a profound effect on the gelation ability of the corresponding bis-amides; while **3,3-Phe** (3-pyridyl bis-amide of L-phenylalanine) was an organogelator, its phenyl analogue (**0,0-Phe**) turned out to be a hydrogelator and was able to gel DMF/water and DMSO/water. In a similar fashion, **3,3-Ala** was a nongelator whereas **0,0-Ala** turned out to be an ambidextrous gelator. The role of the pyridyl moieties in gelation was also probed by pH-dependent gelation experiments (see the Supporting Information). **3,3-Phe** could not gel 1,2-dichlorobenzene below pH 3, thus indicating an active role of the pyridyl moieties. The minimum gelator concentration (MGC) and gel–sol dissociation temperature ( $T_{gel}$ ) were in the range of 0.32–4.0 wt % and 52–110 °C, respectively, thereby indicating the significant gelation efficiency and moderate to excellent thermal stability of the gels. As shown in Figure 2,  $T_{gel}$  gradually increased with an increase in gelator concentration. Such an increase in  $T_{gel}$  may be attributed to the various non-covalent interactions such as hydrogen bonding and hydrophobic interactions that are responsible for forming SAFINs in the gels.

Differential scanning calorimetry (DSC) experiments for two selected gel samples derived from **3,3-Phe** and **3,4-Phe** clearly showed the thermoreversible nature of the gels

Table 1. Gelation data.

Sr. No	Solvent	<b>3,3-Ala</b>		<b>3,4-Ala</b>		<b>3,0-Ala</b>		<b>0,0-Ala</b>		<b>3,3-Phe</b>		<b>3,4-Phe</b>		<b>3,0-Phe</b>		<b>0,0-Phe</b>	
		MGC [wt %]	$T_{gel}$ [°C]	MGC [wt %]	$T_{gel}$ [°C]	MGC [wt %]	$T_{gel}$ [°C]	MGC [wt %]	$T_{gel}$ [°C]	MGC [wt %]	$T_{gel}$ [°C]	MGC [wt %]	$T_{gel}$ [°C]	MGC [wt %]	$T_{gel}$ [°C]	MGC [wt %]	$T_{gel}$ [°C]
1	Acetonitrile	L	–	NC	–	NC	–	FC	–	WP	–	WP <sup>[a]</sup>	–	WP	–	FC	–
2	<i>o</i> -Xylene	L	–	WP	–	2.86	68	4	80	1.22	110	WP <sup>[a]</sup>	–	WP	–	WP	–
3	<i>m</i> -Xylene	L	–	WP	–	1.82	56	GN	–	L	–	WP <sup>[a]</sup>	–	WP	–	WP	–
4	<i>p</i> -Xylene	L	–	WP	–	2.22	70	4	84	L	–	WP <sup>[a]</sup>	–	WP	–	WP	–
5	Chlorobenzene	L	–	WP	–	WP	–	4	78	0.91	67	WP <sup>[a]</sup>	–	WP	–	WP	–
6	1,2-Di chlorobenzene	L	–	WP	–	WP	–	GN	–	0.47	73	2.22	80	WP	–	WP	–
7	Nitrobenzene	L	–	WP	–	WP	–	L	–	WP	–	WP	–	4	52	WP	–
8	Toluene	L	–	WP	–	2.22	66	WP	–	WP	–	WP <sup>[a]</sup>	–	WP	–	WP	–
9	Mesitylene	L	–	NC	–	2.86	58	4	90	WP	–	WP <sup>[a]</sup>	–	WP	–	WP	–
10	Methyl salicylate	L	–	4	90	2.22	62	FC	–	WP	–	WP <sup>[a]</sup>	–	GN	–	WP	–
11	DMSO	L	–	L	–	L	–	4 <sup>[b]</sup>	85	L	–	L	–	WP	–	0.95 <sup>[b]</sup>	80
12	DMF	L	–	L	–	L	–	4 <sup>[b]</sup>	96	L	–	WP <sup>[a]</sup>	–	WP	–	1.5 <sup>[b]</sup>	90
13	EG	L	–	L <sup>[b]</sup>	–	L	–	0.95 <sup>[b]</sup>	78	L	–	L	–	WP	–	0.32 <sup>[b]</sup>	78
14	DEG	L	–	L	–	L	–	4 <sup>[b]</sup>	82	L	–	L	–	WP	–	0.95 <sup>[b]</sup>	94
15	H <sub>2</sub> O	L <sup>[a]</sup>	–	NS	–	NS	–	NS	–	WP <sup>[a]</sup>	–	WP <sup>[a]</sup>	–	NS	–	NS	–

[a] Cosolvent dimethylsulfoxide (minimum) required to dissolve. [b] The corresponding solvents were added to dissolve the gelator in water. L, liquid; FC, fibrous crystal; WP, white precipitate; NC, needle-shaped crystals; GN, gelatinous network; DMSO, dimethylsulfoxide; DMF, *N,N*-dimethylformamide; EG, ethylene glycol; DEG, diethylene glycol; NS, not soluble.

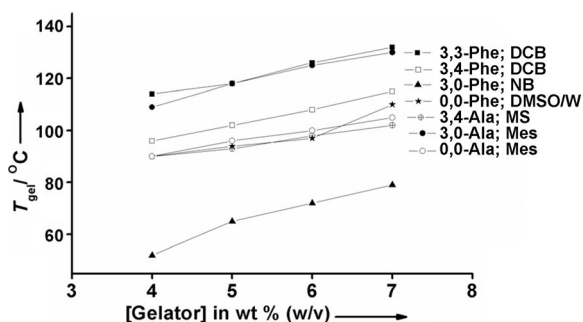


Figure 2. Plot of  $T_{gel}$  as a function of gelator concentration; DCB=1,2-dichlorobenzene; NB= nitrobenzene; DMSO/W = *N,N*-dimethylsulfoxide/water (8:5, v/v); MS= methylsalicylate; Mes= mesitylene.

(Figure 3). The gel-to-sol phase transition temperature found in DSC experiments (129 and 109 °C for the 6 wt.% 1,2-dichlorobenzene (DCB) gel of **3,3-Phe** and **3,4-Phe**, respectively) matched well with the value determined by the dropping ball method (126 and 108 °C, respectively), highlighting that the  $T_{gel}$  data obtained from the dropping ball method could be relied upon in case DSC experiments failed to result in a noticeable phase transition.

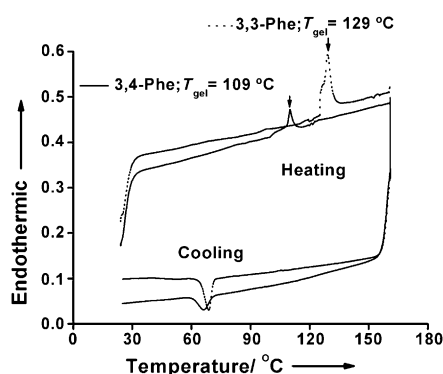


Figure 3. DSC traces of an approximately 6.0 wt.% 1,2-dichlorobenzene gel of **3,3-Phe** and **3,4-Phe**.

To probe the self-assembly process in the gelation process, we performed temperature-variable  $^1\text{H}$ NMR spectroscopy experiments. For this purpose, we chose 2.0 wt.% and 1.54 wt.% (w/v) DMSO/ $\text{H}_2\text{O}$  (1:1 and 5:8 (v/v), respectively) gels of **0,0-Ala** and **0,0-Phe**. In the case of **0,0-Ala**, it was observed that the aromatic protons and the proton attached to the chiral carbon atom gradually shifted downfield (7.3–8.5 and 4.7–5.5 ppm, respectively) with an increase in temperature from 25 to 85 °C, thus signifying that these protons experienced shielding during gelation, which could either be due to C–H $\cdots\pi$  or  $\pi$ – $\pi$  interactions (Figure 4). On the other hand, no such effect was observed in the case of **0,0-Phe**, thereby suggesting that such interactions were not contributing to hydrogelation (see the Supporting Information). These data corroborated well with the single-crystal structures of the analogous molecules (see below).

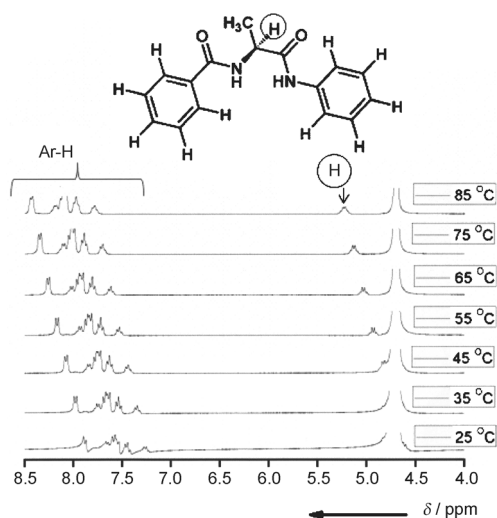


Figure 4. Variable-temperature  $^1\text{H}$ NMR spectra of the hydrogel of **0,0-Ala**.

### Microscopy

Scanning electron microscopy (SEM) micrographs of the xerogels of some selected gels were collected (Figure 5). Most of them showed highly aligned (for **3,0-Ala**, **0,0-Ala**, and **3,0-Phe**) or entangled (for **3,4-Phe**) fibers, whereas one of them (**3,3-Phe**) displayed both fibers and colloidal particles, both of which were also observed in the corresponding transmission electron microscopy (TEM) images (Figure 5). These data clearly indicated that in most of the cases 1D growth of the gel fibers was promoted and accordingly, the solvent molecules were immobilized within the entangled network of fibers resulting in a gel.

### Rheology

Dynamic rheology experiments of a few selected gels (6 wt.% DCB gels of **3,3-Phe** and **3,4-Phe**) were carried out to study the viscoelastic nature or gel-like response of the corresponding gels.<sup>[39]</sup> In a typical frequency sweep experiment, the elastic modulus  $G'$  and loss modulus  $G''$  were plotted as a function of angular frequency ( $\omega$ ) over a significant time period at a constant strain of 0.05 and 0.01 % (as suggested by amplitude sweep experiments, see the Supporting Information); the data for 6 wt.% DCB gels of **3,3-Phe** and **3,4-Phe**, respectively, are shown in Figure 6. The elastic modulus  $G'$  of the gel of **3,3-Phe** was about 3.8 times higher than that of the gel of **3,4-Phe**, thus indicating that a subtle change of the position of the pyridyl N atom had a profound effect on the flow behavior of the gel.

### Self-Sustaining, Load-Bearing, and Self-Healing Experiments

The 1,2-dichlorobenzene gel of **3,3-Phe** was found to be a self-sustaining material even at a concentration as low as 1.0 wt.%. Thus, it could be kept undeformed on a glass slide

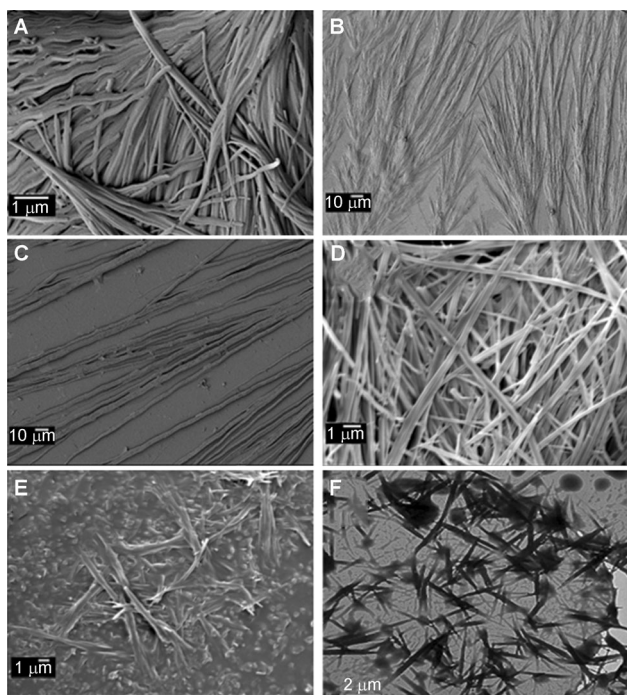


Figure 5. A–E) SEM images of selected xerogels. All xerogels were prepared from the gel of different solvents given within parentheses. A) **3,0-Ala** (*o*-xylene); B) **0,0-Ala** [DMSO/H<sub>2</sub>O (37%)]; C) **3,0-Phe** (nitrobenzene); D) **3,4-Phe** (nitrobenzene); and E) **3,3-Phe** (1,2-dichlorobenzene). F) TEM image of the xerogel of **3,3-Phe** prepared from 1,2-dichlorobenzene.

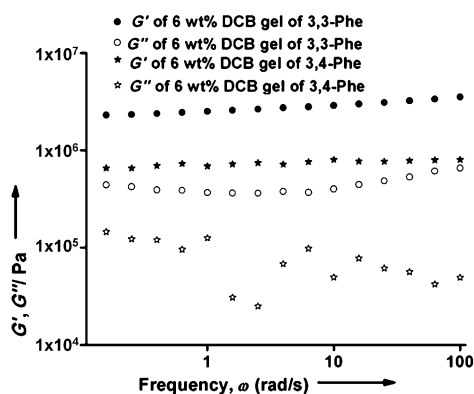


Figure 6. Dynamic rheology of a 6 wt.% DCB gel of **3,3-Phe** and **3,4-Phe** at 25°C. The elasticity modulus  $G'$  and viscosity modulus  $G''$  are shown as a function of the angular frequency  $\omega$ . The strain used was 0.1%; DCB = 1,2-dichlorobenzene.

without any container. The self-sustaining behavior of this gel was also demonstrated by carving the word ‘IACS’ on a slice of the gel (1.0 wt.% DCB gel). The load-bearing ability of this gel (2.5 mL) was also extraordinary: 14 Indian 5 Rupee coins weighing 125.0 g could be kept on a cylindrical piece (1.0×0.9 cm) of this gel with no visible deformation or solvent leaching. This gel also displayed highly efficient self-healing properties; when a slab (3.0×1.1×0.3 cm) was cut

into 4 pieces and allowed to self-heal, the pieces formed a single piece within 15 min (Figure 7). Unfortunately, none of the gels prepared from other compounds in the series showed any self-sustaining, load-bearing, and self-healing properties.

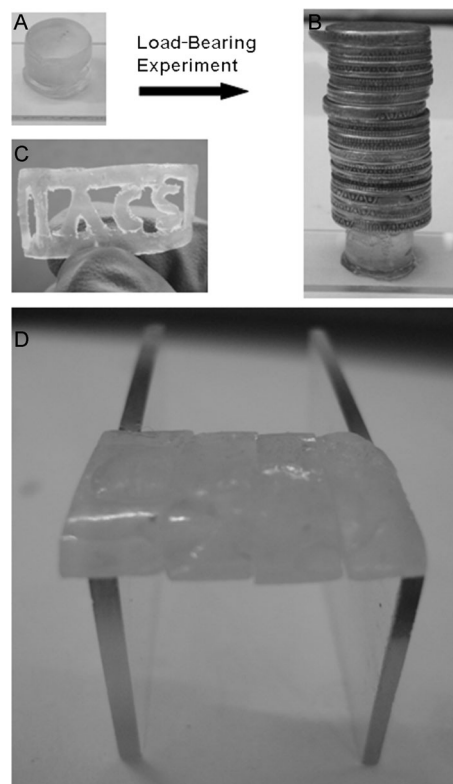


Figure 7. A) Free-standing and B) load-bearing DCB gel (1 wt %) of **3,3-Phe**. C) Gel slice with the abbreviation ‘IACS’ carved. D) Self-healing of several gel blocks of **3,3-Phe**.

### Structure–Property Correlation

A detailed insight into the structure is the key to any design aspect. Thus, it is highly desirable and important to understand the detailed structure of the gel network or SAFINs. However, determination of the structure of SAFINs is challenging; understandably, single-crystal X-ray diffraction is not an option because of the submicron size of the gel fibers. To determine the structure of the gel fiber in a gel sample, ab initio structure determination from diffraction data of a gel sample collected in a synchrotron beam-line should be employed. However, limited access to such a beam-line and the non-routine nature of ab initio structure determination from powder X-ray diffraction (PXRD) data<sup>[40]</sup> compelled researchers to develop other, relatively easy alternative avenues. Thus, an indirect method was developed originally by Weiss et al.,<sup>[41]</sup> wherein the various powder X-ray diffraction patterns (PXRDs) (simulated from single-crystal X-ray data, bulk solid, gels/xerogels) are compared; a near perfect match of these patterns would indirectly determine the structure of the SAFINs. In principle,

the comparison of these PXRDs should be strictly restricted to simulated, bulk, and gel. However, obtaining a meaningful PXRD pattern for a gel sample is often difficult because of the scattering contribution of the solvent and the generally poor diffraction (due to low crystallinity and/or a low amount of the gelator present in a gel). On the other hand, during xerogel formation (usually done by evaporating a gel sample), a new nucleation event might occur from the already dissolved gelator molecules present in the bulk solvent of a gel, thus leading to a mismatch of the PXRD patterns due to the formation of a new crystalline phase. However, there is no guarantee that such an event would always take place. Thus, comparing simulated, bulk solid, and xerogel PXRD patterns is a reasonable compromise in determining the gel network structure. Our best efforts resulted in crystallization of two gelator molecules, namely **3,3-Phe** and **3,4-Ala**, which were subjected to SXRD.

The crystals of **3,3-Phe** were grown from a DMSO/water (1:5, v/v) mixture and were crystallized in the noncentrosymmetric monoclinic space group  $P2_1$  (Table 2). The asymmetric unit contained two molecules of **3,3-Phe**. The dihedral angles between the two pyridyl moieties in these molecules were 63.2 and 61.2°. Contrary to general wisdom, the pyridyl N atoms did not participate in hydrogen bonding whereas the amide functionalities, as expected, displayed

a beta-sheet-like hydrogen bond network through N–H⋯O interactions [ $N\cdots O = 2.977(4)–3.017(4)$  Å;  $\angle N–H\cdots O = 156(3)–161(3)^\circ$ ], thereby leading to a 1D hydrogen-bonded strand. Such 1D strands were further packed in a parallel fashion (Figure 8).

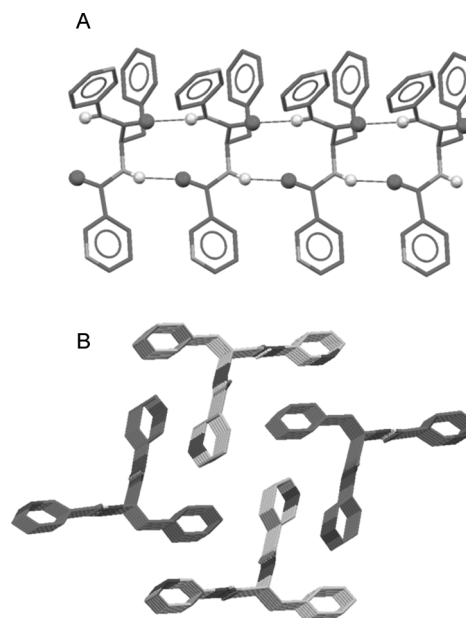


Figure 8. Illustration of the crystal structure of **3,3-Phe**; 1D hydrogen bond network through N–H⋯O interactions (A) and overall parallel packing (B). All hydrogen atoms (except N–H) were omitted for clarity.

Table 2. Crystallographic parameters.

Crystallographic parameters	<b>3,4-Ala</b>	<b>3,3-Phe</b>
Empirical formula	C <sub>14</sub> H <sub>14</sub> N <sub>4</sub> O <sub>2</sub>	C <sub>20</sub> H <sub>18</sub> N <sub>4</sub> O <sub>2</sub>
CCDC No.	953874	953873
Formula weight	270.29	246.38
Crystal size/mm	0.20 × 0.16 × 0.08	0.24 × 0.18 × 0.12
Crystal system	Monoclinic	Monoclinic
Space group	$P2_1$	$P2_1$
<i>a</i> [Å]	7.9724(5)	17.9316(17)
<i>b</i> [Å]	8.8830(5)	5.1648(5)
<i>c</i> [Å]	9.6390(6)	18.9905(19)
$\alpha$ [°]	90.00	90.00
$\beta$ [°]	110.274(2)	103.643(3)
$\gamma$ [°]	90.00	90.00
Volume [Å <sup>3</sup> ]	640.33(7)	1709.1(3)
<i>Z</i>	2	4
<i>D</i> <sub>calc</sub> [g cm <sup>-3</sup> ]	1.402	1.346
<i>F</i> (000)	284	728
$\mu$ MoK $\alpha$ [mm <sup>-1</sup> ]	0.098	0.090
<i>T</i> [K]	298(2)	298(2)
<i>R</i> <sub>int</sub>	0.0196	0.0345
Range of <i>h, k, l</i>	–8/8, –8/9, –9/9	–20/20, –6/5, –22/22
$\theta_{\min/\max}$ [°]	2.25/22.47	1.10/24.45
Reflections collected/unique/observed	4823/866/861	15254/3154/2660
[ <i>I</i> > 2 $\sigma$ ( <i>I</i> )]		
Data/restraints/parameters	866/1/182	3154/1/485
Goodness of fit on <i>F</i> <sup>2</sup>	1.082	1.038
Final <i>R</i> indices [ <i>I</i> > 2 $\sigma$ ( <i>I</i> )]	<i>R</i> <sub>1</sub> = 0.0235 <i>wR</i> <sub>2</sub> = 0.0584	<i>R</i> <sub>1</sub> = 0.0410 <i>wR</i> <sub>2</sub> = 0.1063
<i>R</i> indices (all data)	<i>R</i> <sub>1</sub> = 0.0236 <i>wR</i> <sub>2</sub> = 0.0585	<i>R</i> <sub>1</sub> = 0.0504 <i>wR</i> <sub>2</sub> = 0.1141

The crystals of **3,4-Ala** were grown from an acetonitrile/water (1:20, v/v) mixture and were found to be in the noncentrosymmetric monoclinic space group  $P2_1$  (Table 2). The asymmetric unit contained one molecule of **3,4-Ala**. The dihedral angle between the two pyridyl moieties was 88.6°, that is, they are almost orthogonal to each other. Unlike **3,3-Phe**, one of the pyridyl N atoms participated in hydrogen bonding with one of the amide moieties through N–H⋯N interactions [ $N\cdots N = 2.967(3)$  Å;  $\angle N–H\cdots N = 174.2^\circ$ ]; the other amide moiety displayed the usual amide⋯amide hydrogen bonding through N–H⋯O interactions [ $N\cdots O = 2.871(2)$  Å;  $\angle N–H\cdots O = 170.0^\circ$ ], thus resulting in an overall 2D HBN. In this case, C–H⋯ $\pi$  interactions (3.249 and 3.386 Å) were also observed (Figure 9). It may be noted here that the temperature-variable <sup>1</sup>H NMR data (see above) of an analogous compound, namely **0,0-Ala**, displayed C–H⋯ $\pi$  or  $\pi$ – $\pi$  interactions.

We carried out PXRD experiments on selected gels of **3,3-Phe** and **3,4-Ala** as depicted in Figure 10. It was clear from the plots that in the case of **3,4-Ala** the PXRD patterns obtained under various conditions were nearly superimposable, which meant that the single-crystal structure in this case actually represented the bulk as well as the SAFINs found in the xerogels. However, in the case of **3,3-Phe**, the PXRD patterns of the bulk and simulated matched very well but did not match with the PXRD pattern of the

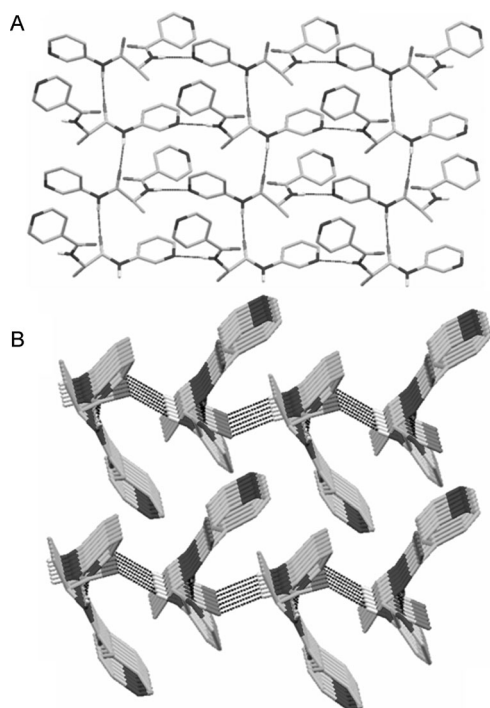


Figure 9. Illustration of the crystal structure of **3,4-Ala**: 2D hydrogen bond network through N–H...O and N–H...N interactions (A) and overall parallel packing (B). All hydrogen atoms (except N–H) were omitted for clarity.

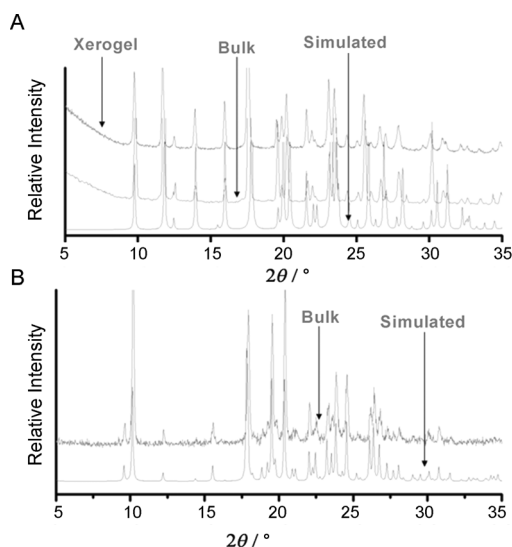


Figure 10. PXRD patterns of **3,4-Ala** (A) and **3,3-Phe** (B) under various conditions.

xerogels, which meant the existence of a new crystalline phase other than the phase present in the single crystal.

## Conclusions

A new series of bis-amides of L-alanine and L-phenyl alanine have been synthesized by considering various combina-

tion of pyridyl and phenyl moieties as terminal groups as potential low-molecular-weight gelators. Out of the 8 bis-amides synthesized, 7 turned out to be gelators of both organic and aqueous solvents. Both 1D and 2D hydrogen bond networks could be seen in the single-crystal structures of two gelator molecules (**3,3-Phe** and **3,4-Ala**, respectively), thus indicating the importance of 1D and 2D hydrogen bond networks in gelation. Temperature-variable  $^1\text{H}$  NMR experiments on one such gel (**0,0-Ala**) confirmed the presence of either  $\pi$ - $\pi$  or C–H... $\pi$  interactions during gelation, in good agreement with the single-crystal structure of an analogous gelator (**3,4-Ala**). Remarkably, a 1,2-dichlorobenzene gel of **3,3-Phe** displayed excellent shape-sustaining, load-bearing, and self-healing properties, which are not so common in supramolecular gels.

## Experimental Section

### Materials and Physical Measurements

All the starting materials and reagents were commercially available and were used without further purification. Solvents were of LR grade and used without further distillation. Both  $^1\text{H}$  and  $^{13}\text{C}$  NMR spectra were collected using a 500 MHz spectrometer (Bruker Ultrashield Plus-500) and a 300 MHz spectrometer (Bruker Avance DPX-300). FT-IR spectra were obtained using an FTIR instrument (FTIR-8300, Shimadzu). The elemental compositions of all the purified compounds were confirmed by elemental analysis using a PerkinElmer 2400, Series-II, CHNO/S elemental analyzer. SEM images of the selected xerogels were recorded using a JEOL JMS-6700F field-emission scanning electron microscope. TEM images of selected samples were recorded by using a JEOL instrument and a 300 mesh copper TEM grid. DSC data were recorded using PerkinElmer Diamond DSC system. All the rheology studies were carried out using an SDT Q series advanced rheometer AR 2000. X-ray powder diffraction patterns were recorded using a Bruker AXS D8 Advance powder X-ray diffractometer ( $\text{Cu}_{\text{K}\alpha 1}$  radiation).

### Measurements of the Gel-Sol Dissociation Temperature ( $T_{\text{gel}}$ )

$T_{\text{gel}}$  values were determined using the dropping ball method. A locally made glass ball that weighed 306.0 mg was kept on the top of the gel (0.5 mL) prepared in a test tube (10×100 mm). The tube was immersed in an oil bath and then placed on a magnetic stirrer to ensure uniform heating. The temperature at which the ball reached the bottom of the tube was considered to be  $T_{\text{gel}}$ .

### SEM and TEM Imaging

Dilute (0.3–0.5 wt. %) solutions of the corresponding gelators were drop-cast on a glass plate fixed with a standard metallic SEM stub and allowed to dry under ambient conditions. All the samples were coated with platinum prior to recording of SEM images. The sample for TEM was prepared by depositing a drop of a dilute solution (on the order of  $\sim 10^{-3}$  M) on a carbon-coated Cu (300 mesh) TEM grid. Subsequently, the grid was dried under vacuum at room temperature overnight and used for recording TEM images using an accelerating voltage of 200 kV.

### Single-Crystal X-ray Diffraction

Single crystals suitable for X-ray diffraction were obtained by slow evaporation at room temperature from the corresponding solvent systems mentioned in the structure descriptions. Single-crystal X-ray data were collected with  $\text{Mo}_{\text{K}\alpha}$  radiation ( $\lambda = 0.7107 \text{ \AA}$ ) using a SMART APEX-II diffractometer equipped with a CCD area detector. All the data collection, data reduction, and structure solution and refinement were carried out using the SMART APEX-II software package. All the structures were solved by direct methods and refined in a routine manner. In all

cases, non-hydrogen atoms were treated anisotropically. Whenever possible, the hydrogen atoms were located on a difference Fourier map and refined. In other cases, the hydrogen atoms were geometrically fixed at their idealized positions. CCDC 953873 (**3,3-Phe**) and CCDC 953874 (**3,4-Ala**) contain the supplementary crystallographic data for this paper. These data can be obtained free of charge from The Cambridge Crystallographic Data Centre via [www.ccdc.cam.ac.uk/data\\_request/cif](http://www.ccdc.cam.ac.uk/data_request/cif).

#### Synthesis Procedure

Pyridin-3-amine (0.72 g, 7.5 mmol) was dissolved in dry THF (50 mL) in a 250 mL two-neck round-bottomed flask under nitrogen atmosphere and then DCC (1.53 g, 7.5 mmol, 1 equiv) was added. Subsequently, a pre-prepared solution of N-Boc-L-alanine (1.42 g, 7.5 mmol, 1 equiv) or phenylalanine (2 g, 7.5 mmol, 1 equiv) in dry THF (50 mL) was added slowly to the amine solution cooled in an ice bath and stirred overnight. The reaction mixture was then filtered and the filtrate evaporated under reduced pressure to afford a white residue (compound 1). This residue was dissolved in a 15% acidic solution (HCl/dry methanol, v/v) and stirred overnight. Subsequently, dry Et<sub>2</sub>O was added to yield white crystals (compound 2), which were then dissolved in CH<sub>2</sub>Cl<sub>2</sub> through the addition of dry triethylamine. One equivalent of acid chloride was dissolved in dry CH<sub>2</sub>Cl<sub>2</sub> with the addition of dry triethylamine and added to the solution of compound 2 in CH<sub>2</sub>Cl<sub>2</sub>. Following stirring for overnight, the compounds were purified by column chromatography (methanol/chloroform, 1:50) to afford the product as a white powder.

**3,3-Phe**: m.p. = 176 °C; <sup>1</sup>H NMR (300 MHz, [D<sub>6</sub>]DMSO): δ = 10.44 (s, 1H), 9.08–9.02 (d, J = 8.1 Hz, 1H), 8.94 (s, 1H), 8.74 (s, 1H), 8.72–8.65 (d, J = 3.6 Hz, 1H), 8.30–8.23 (d, J = 3.6 Hz, 1H), 8.17–8.10 (d, J = 7.8 Hz, 1H), 8.06–7.99 (d, J = 7.8 Hz, 1H), 7.52–7.44 (dd, J = 7.8 Hz, J = 4.8 Hz, 1H), 7.43–7.30 (m, 3H), 7.30–7.22 (t, J = 7.2 Hz, 2H), 7.22–7.12 (t, J = 7.2 Hz, 2H), 4.93–4.80 (m, 1H), 3.25–3.00 ppm (m, 2H.); <sup>13</sup>C NMR (300 MHz, [D<sub>6</sub>]DMSO): δ = 171.26, 165.68, 152.61, 152.53, 149.17, 149.06, 144.99, 141.62, 141.52, 138.33, 135.96, 135.72, 129.87, 129.72, 128.69, 126.99, 124.17, 123.91, 56.26, 37.65 ppm; FT-IR (KBr pellet):  $\tilde{\nu}$  = 3345, 1655, 1599, 1578, 1533, 1495, 1439, 1323, 750, 716, 691 cm<sup>-1</sup>; elemental anal. calc. (%) for C<sub>20</sub>H<sub>18</sub>N<sub>2</sub>O<sub>2</sub>: C 69.35, H 5.24, N 16.17; found: C 69.26, H 5.34, N 15.97; MS: *m/z* (%): 347 [M+H]<sup>+</sup> (100), 369 [M+Na]<sup>+</sup> (40).

**3,4-Phe**: m.p. = 160 °C; <sup>1</sup>H NMR (500 MHz, [D<sub>6</sub>]DMSO): δ = 10.46 (s, 1H), 9.17–9.12 (d, J = 8.0 Hz, 1H), 8.77 (s, 1H), 8.75–8.71 (m, 2H), 8.32–8.28 (d, J = 4.5 Hz, 1H), 8.08–8.03 (d, J = 8.0 Hz, 1H), 7.77–7.72 (m, 2H), 7.44–7.35 (m, 3H), 7.33–7.27 (t, J = 8.0, 2H), 7.23–7.17 (t, J = 7.5 Hz, 1H), 4.94–4.87 (m, 1H), 3.25–3.19 (dd, J = 4.5 Hz, J = 9.0 Hz, 1H); <sup>13</sup>C NMR (500 MHz, [D<sub>6</sub>]DMSO): δ = 170.46, 164.95, 150.10, 144.41, 141.01, 140.67, 137.65, 135.32, 129.09, 128.07, 126.38, 123.55, 121.31, 55.66, 36.10 ppm; FT-IR (KBr pellet):  $\tilde{\nu}$  = 3300, 1670, 1637, 1605, 1553, 1529, 1483, 1431, 1292, 696 cm<sup>-1</sup>; elemental anal. calc. (%) for C<sub>20</sub>H<sub>18</sub>N<sub>2</sub>O<sub>2</sub>: C 69.35, H 5.24, N 16.17; found: C 68.64, H 5.19, N 16.01; MS: *m/z* (%): 347 [M+H]<sup>+</sup> (100), 369 [M+Na]<sup>+</sup> (40).

**3,0-Phe**: m.p. = 156 °C; <sup>1</sup>H NMR (500 MHz, [D<sub>6</sub>]DMSO): δ = 10.42 (s, 1H), 8.80–8.75 (m, 2H), 8.30–8.26 (d, J = 4.5 Hz, 1H), 8.06–8.03 (d, J = 8.5 Hz, 1H), 7.85–7.83 (d, J = 7.5 Hz, 2H), 7.55–7.51 (t, J = 7.5 Hz, 1H), 7.48–7.44 (t, J = 7.5 Hz, 2H), 7.42–7.40 (d, J = 7.5 Hz, 2H), 7.37–7.34 (q, J = 8.5 Hz, J = 4.5 Hz, 1H), 7.31–7.27 (t, J = 7.5 Hz, 2H), 7.21–7.17 (t, J = 7.5 Hz, 1H), 4.90–4.85 (m, 1H), 3.21–3.10 ppm (m, 2H.); <sup>13</sup>C NMR (500 MHz, [D<sub>6</sub>]DMSO): δ = 171.57, 167.09, 144.93, 141.56, 138.52, 136.05, 134.38, 131.93, 129.73, 128.73, 128.66, 126.93, 126.90, 124.16, 56.32, 37.62 ppm; FT-IR (KBr pellet):  $\tilde{\nu}$  = 3300, 1672, 1549, 1485, 1288, 702 cm<sup>-1</sup>; elemental anal. calc. (%) for C<sub>20</sub>H<sub>17</sub>N<sub>3</sub>O<sub>2</sub>: C 72.49, H 5.17, N 12.68; found: C 72.92, H 5.66, N 11.95; MS: *m/z* (%): 346 [M+H]<sup>+</sup> (100), 368 [M+Na]<sup>+</sup> (40).

**0,0-Phe**: m.p. = 162 °C; <sup>1</sup>H NMR (500 MHz, [D<sub>6</sub>]DMSO): δ = 10.22 (s, 1H), 8.80–8.70 (d, J = 8 Hz, 1H), 7.90–7.80 (d, J = 7 Hz, 2H), 7.68–7.60 (d, J = 8 Hz, 2H), 7.56–7.50 (t, J = 7, 1H), 7.49–7.48 (m, 4H), 7.40–7.27 (m, 4H), 7.20–7.16 (t, J = 7.5, 1H), 7.04–7.50 (t, J = 7.5, 1H), 4.90–4.83 (m, 1H), 3.20–3.06 ppm (m, 2H); <sup>13</sup>C NMR (500 MHz, [D<sub>6</sub>]DMSO): δ = 170.97, 167.02, 139.45, 138.68, 134.47, 131.88, 129.76, 129.26, 128.72, 128.62, 128.00, 126.87, 123.92, 119.91, 56.35, 37.75 ppm; FT-IR (KBr pellet):  $\tilde{\nu}$  =

3289, 1667, 1638, 1533, 1445, 690 cm<sup>-1</sup>; elemental anal. calc. (%) for C<sub>22</sub>H<sub>20</sub>N<sub>2</sub>O<sub>2</sub>: C 76.72, H 5.85, N 8.13; found: C 76.60, H 5.82, N 7.93; MS: *m/z* (%): 367 [M+Na]<sup>+</sup> (100).

**3,3-Ala**: <sup>1</sup>H NMR (300 MHz, MeOD-d<sub>4</sub>): δ = 9.04 (s, 1H), 8.76 (s, 1H), 8.72–8.58 (d, J = 4.8 Hz, 1H), 8.32–8.13 (m, 2H), 8.13–7.92 (d, J = 8.97 Hz, 1H), 7.56–7.40 (dd, J = 7.8, J = 4.8, 1H), 7.40–7.10 (dd, J = 7.8, J = 4.8, 1H), 4.76–4.64 (q, 1H), 1.59–1.57 ppm (d, J = 7.2 Hz, 3H); <sup>13</sup>C NMR (300 MHz, MeOD-d<sub>4</sub>): δ = 173.95, 167.90, 152.79, 149.43, 145.35, 142.01, 137.30, 131.43, 129.17, 125.0, 125.31, 125.09, 51.9, 17.83 ppm; FT-IR (KBr pellet):  $\tilde{\nu}$  = 3269, 1643, 1547, 1482, 1421, 1286, 706 cm<sup>-1</sup>; MS: *m/z* (%): 271 [M+H]<sup>+</sup> (45), 293 [M+Na]<sup>+</sup> (100).

**3,0-Ala**: m.p. = 138 °C; <sup>1</sup>H NMR (500 MHz, [D<sub>6</sub>]DMSO): δ = 10.28 (s, 1H), 8.79–8.76 (d, J = 2 Hz, 1H), 8.79–8.76 (d, J = 6.5 Hz, 1H), 8.28–8.25 (d, J = 4.5 Hz, 1H), 8.08–8.04 (d, J = 8.5 Hz, 1H), 7.94–7.91 (d, J = 7.0 Hz, 2H), 7.57–7.53 (t, J = 7.0 Hz, 1H), 7.50–7.46 (t, J = 7.5 Hz, 2H), 4.65–4.59 (m, 1H), 3.47–3.43 ppm (d, J = 7.5, 3H); <sup>13</sup>C NMR (500 MHz, [D<sub>6</sub>]DMSO): δ = 172.61, 166.89, 144.76, 141.45, 136.28, 134.42, 131.90, 128.72, 128.10, 126.72, 124.13, 50.42, 18.15 ppm; FT-IR (KBr pellet):  $\tilde{\nu}$  = 3308, 3262, 1668, 1609, 1553, 1425, 1325, 1194, 837, 509 cm<sup>-1</sup>; elemental anal. calc. (%) for C<sub>15</sub>H<sub>15</sub>N<sub>3</sub>O<sub>2</sub>: C 66.90, H 5.61, N 15.60; found: C 66.83, H 5.42, N 15.27; MS: *m/z* (%): 270 [M+H]<sup>+</sup> (100), 292 [M+Na]<sup>+</sup> (60).

**3,4-Ala**: m.p. = 154 °C; <sup>1</sup>H NMR (300 MHz, [D<sub>6</sub>]DMSO): δ = 10.29 (s, 1H), 9.04–8.96 (d, J = 6.6 Hz, 1H), 8.78–8.69 (t, J = 5.4 Hz, 3H), 8.28–8.23 (d, J = 4.5 Hz, 1H), 8.00–8.07 (d, J = 8.1 Hz, 1H), 7.84–7.78 (d, J = 4.8 Hz, 2H), 7.38–7.30 (q, J = 5.1 Hz, 1H), 4.66–4.56 (t, J = 7.2 Hz, 1H), 1.48–1.40 ppm (d, J = 6.6, 3H.); <sup>13</sup>C NMR (300 MHz, [D<sub>6</sub>]DMSO): δ = 172.24, 165.47, 150.78, 144.92, 141.40, 136.26, 126.86, 124.25, 122.13, 50.57, 18.12 ppm; FT-IR (KBr pellet):  $\tilde{\nu}$  = 3254, 1678, 1657, 1541, 1485, 1329, 1287, 638 cm<sup>-1</sup>; elemental anal. calc. (%) for C<sub>14</sub>H<sub>14</sub>N<sub>4</sub>O<sub>2</sub>: C 62.21, H 5.22, N 20.73; found: C 63.12, H 5.14, N 20.33; MS: *m/z* (%): 270.85 [M+H]<sup>+</sup> (100), 292.8 [M+Na]<sup>+</sup> (30).

**0,0-Ala**: m.p. = 145 °C; <sup>1</sup>H NMR (500 MHz, MeOD-d<sub>4</sub>): δ = 10.03 (s, 1H), 8.64–8.56 (d, J = 11.5 Hz, 1H), 7.93–7.85 (d, J = 11.5 Hz, 2H), 7.57–7.49 (m, 5H), 7.35–7.20 (t, J = 13, 2H), 7.09–6.95 (t, J = 12.5, 1H), 4.68–4.54 (m, 1H), 3.19–3.11 (d, J = 9 Hz, 1H), 1.49–1.35 ppm (d, J = 12 Hz, 3H); <sup>13</sup>C NMR (300 MHz, MeOD-d<sub>4</sub>): δ = 171.92, 166.71, 139.55, 134.38, 131.77, 129.12, 128.62, 127.98, 123.63, 119.63, 50.33, 18.25 ppm; FT-IR (KBr pellet):  $\tilde{\nu}$  = 2893, 1668, 1601, 1582, 1537, 1522, 1445, 1256, 1117, 752, 696 cm<sup>-1</sup>; elemental anal. calc. (%) for C<sub>16</sub>H<sub>16</sub>N<sub>2</sub>O<sub>2</sub>: C 71.62, H 6.01, N 10.44; found: C 72.20, H 6.50, N 9.85; MS: *m/z* (%): 291 [M+Na]<sup>+</sup> (100).

## Acknowledgements

U.K.D. and P.D. thank CSIR, New Delhi for their Senior Research Fellowship (SRF) and financial support, respectively. S.B. thanks IACS for his Senior Research Fellowship (SRF). All the single-crystal X-ray diffraction data were collected at the DBT funded Single Crystal Diffractometer facility at the Department of Organic Chemistry, IACS, Kolkata.

- [1] a) P. Terech, R. G. Weiss, *Chem. Rev.* **1997**, 97, 3133–3160; b) *Molecular Gels: Materials with Self-Assembled Fibrillar Networks* (Eds.: R. G. Weiss, P. Terech), Springer, Dordrecht, **2005**.
- [2] a) A. Ballabh, D. R. Trivedi, P. Dastidar, *Chem. Mater.* **2006**, 18, 3795–3800; b) S. Bhattacharya, Y. K. Ghosh, *Chem. Commun.* **2001**, 185–186; c) S. R. Jadhav, P. K. Vemula, R. Kumar, S. R. Raghavan, G. John, *Angew. Chem. Int. Ed.* **2010**, 49, 7695–7698; *Angew. Chem.* **2010**, 122, 7861–7864.
- [3] a) K. Murata, M. Aoki, T. Nishi, A. Ikeda, S. Shinkai, *J. Chem. Soc. Chem. Commun.* **1991**, 1715–1718; b) J. J. D. de Jong, L. N. Lucas, R. M. Kellogg, J. H. van Esch, B. L. Feringa, *Science* **2004**, 304, 278–281.
- [4] E. Carretti, L. Dei in *Molecular Gels: Materials with Self-Assembled Fibrillar Networks* (Eds.: G. Weiss, P. Terech), Springer, Dordrecht, **2005**, Chap. 27, pp. 929–938.

- [5] a) T. Kato, *Science* **2002**, 295, 2414–2418; b) A. Ajayaghosh, V. K. Praveen, C. Vijayakumar, S. George, *Angew. Chem. Int. Ed.* **2007**, 46, 6260–6265; *Angew. Chem.* **2007**, 119, 6376–6381; c) A. Ajayaghosh, C. Vijayakumar, V. K. Praveen, S. Santhosh Babu, R. Varghese, *J. Am. Chem. Soc.* **2006**, 128, 7174–7175.
- [6] a) A. Wynne, M. Whitefield, A. J. Dixon, S. Anderson, *J. Dermatol. Treat.* **2002**, 13, 61–66; b) V. Jennings, A. Gysler, M. Schafer-Korting, S. H. Gohla, *Eur. J. Pharm. Biopharm.* **2000**, 49, 211–218.
- [7] a) K. J. C. van Bommel, A. Friggeri, S. Shinkai, *Angew. Chem. Int. Ed.* **2003**, 42, 980–999; *Angew. Chem.* **2003**, 115, 1010–1030; b) H. Basit, A. Pal, S. Sen, S. Bhattacharya, *Chem. Eur. J.* **2008**, 14, 6534–6545; c) S. Ray, A. K. Das, A. Banerjee, *Chem. Commun.* **2006**, 2816–2818; d) G. Gundiah, S. Mukhopadhyay, U. G. Tumkurkar, A. Govindaraj, U. Maitra, C. N. R. Rao, *J. Mater. Chem.* **2003**, 13, 2118–2122.
- [8] B. Escuder, F. R. Llansola, J. F. Miravet, *New J. Chem.* **2010**, 34, 1044–1054.
- [9] Z. Yang, G. Liang, L. Wang, B. Xu, *J. Am. Chem. Soc.* **2006**, 128, 3038–3043.
- [10] K. Y. Lee, D. J. Mooney, *Chem. Rev.* **2001**, 101, 1869–1880.
- [11] J. A. Foster, M.-O. M. Piepenbrock, G. O. Lloyd, N. Clarke, J. A. K. Howard, J. W. Steed, *Nat. Chem.* **2010**, 2, 1037–1043.
- [12] P. Mukhopadhyay, N. Fujita, A. Takada, T. Kishida, M. Shirakawa, S. Shinkai, *Angew. Chem. Int. Ed.* **2010**, 49, 6338–6342; *Angew. Chem.* **2010**, 122, 6482–6486.
- [13] A. Vidyasagar, K. Handore, K. M. Sureshan, *Angew. Chem. Int. Ed.* **2011**, 50, 8021–8024; *Angew. Chem.* **2011**, 123, 8171–8174.
- [14] Q. Wang, J. L. Mynar, M. Yoshida, E. Lee, M. Lee, K. Okuro, K. Kinbara, T. Aida, *Nature* **2010**, 463, 339–343.
- [15] A. B. W. Brochu, S. L. Craig, W. M. Reichert, *J. Biomed. Mater. Res. Part A* **2011**, 96, 492–506.
- [16] M. Chiesa, P. P. Cardenas, F. Ot'on, J. Martinez, M. Mas-Torrent, F. Garcia, J. C. Alonso, C. Rovira, R. Garcia, *Nano Lett.* **2012**, 12, 1275–1281.
- [17] E. D. Rodriguez, X. Luo, P. T. Mather, *ACS Appl. Mater. Interfaces* **2011**, 3, 152–161.
- [18] F. Y. Liu, F. Y. Li, G. H. Deng, Y. M. Chen, B. Q. Zhang, J. Zhang, C. Y. Liu, *Macromolecules* **2012**, 45, 1636–1645.
- [19] K. Itoga, M. Yamato, J. Kobayashi, A. Kikuchi, T. Okano, *Biomaterials* **2004**, 25, 2047–2053.
- [20] J. Nji, G. Q. Li, *Polymer* **2010**, 51, 6021–6029.
- [21] X. D. Yu, X. H. Cao, L. M. Chen, H. C. Lan, B. Liu, T. Yi, *Soft Matter* **2012**, 8, 3329–3334.
- [22] J. A. Syrett, C. R. Becer, D. M. Haddleton, *Polym. Chem.* **2010**, 1, 978–987.
- [23] P. Dastidar, *Chem. Soc. Rev.* **2008**, 37, 2699–2715.
- [24] a) K. Hanabusa, K. Shimura, K. Hirose, M. Yamada, H. Shirai, *Chem. Lett.* **1996**, 885–886; b) H. Shi, Z. Huang, S. Kilic, J. Xu, R. M. Enick, E. J. Beckman, A. J. Carr, R. E. Melendez, A. D. Hamilton, *Science* **1999**, 286, 1540–1543; c) J. H. van Esch, S. De Feyter, R. M. Kellogg, F. De Schryver, B. L. Feringa, *Chem. Eur. J.* **1997**, 3, 1238–1243.
- [25] a) E. J. de Vries, R. M. Kellogg, *J. Chem. Soc. Chem. Commun.* **1993**, 238–240; b) K. Hanabusa, J. Tange, Y. Taguchi, T. Koyama, H. Shirai, *J. Chem. Soc. Chem. Commun.* **1993**, 390–392; c) A. Aggeli, M. Bell, N. Boden, J. N. Keen, P. F. Knowles, T. C. B. McLeish, M. Pitkeathly, S. E. Radford, *Nature* **1997**, 386, 259–262.
- [26] a) S. Yamamoto, *J. Soc. Chem. Ind. Jpn.* **1943**, 46, 279–281 (CA46:7047h); b) F. R. Tavel, B. Pfannemueller, *Makromol. Chem.* **1990**, 191, 3097–3106; c) S. Yamasaki, H. Tsutsumi, *Bull. Chem. Soc. Jpn.* **1994**, 67, 2053–2056; d) R. J. H. Hafkamp, M. C. Feiters, R. J. M. Nolte, *J. Org. Chem.* **1999**, 64, 412–426; e) U. Beginn, S. Keinath, M. Mçller, *Macromol. Chem. Phys.* **1998**, 199, 2379–2384; f) K. Yoza, N. Amanokura, Y. Ono, T. Akao, H. Shinmori, S. Shinkai, D. N. Reinhoudt, *Chem. Eur. J.* **1999**, 5, 2722–2729.
- [27] a) Y.-C. Lin, R. G. Weiss, *Macromolecules* **1987**, 20, 414–417; b) R. Mukkamala, R. Weiss, *Langmuir* **1996**, 12, 1474–1482; c) C. Geiger, M. Stabescu, L. Chen, D. G. Whitten, *Langmuir* **1999**, 15, 2241–2245.
- [28] a) W. Gu, L. Lu, G. B. Chapman, R. G. Weiss, *Chem. Commun.* **1997**, 543–544; b) R. Oda, I. Huc, S. Candau, *Angew. Chem. Int. Ed.* **1998**, 37, 2689–2691; *Angew. Chem.* **1998**, 110, 2835–2838.
- [29] H. Engelkamp, S. Middelbeck, R. J. M. Nolte, *Science* **1999**, 284, 785–788.
- [30] P. Terech, P. Gebel, R. Ramasseul, *Langmuir* **1996**, 12, 4321–4323.
- [31] C. Geiger, M. Stabescu, L. Chen, D. G. Whitten, *Langmuir* **1999**, 15, 2241–2245.
- [32] M. George, R. G. Weiss, *Acc. Chem. Res.* **2006**, 39, 489–497.
- [33] K. J. C. van Bommel, C. van der Pol, I. Muizebelt, A. Friggeri, A. Heeres, A. Meetsma, B. L. Feringa, J. van Esch, *Angew. Chem. Int. Ed.* **2004**, 43, 1663–1667; *Angew. Chem.* **2004**, 116, 1695–1699.
- [34] P. Sahoo, D. K. Kumar, S. R. Raghavan, P. Dastidar, *Chem. Asian J.* **2011**, 6, 1038–1047.
- [35] P. Sahoo, V. G. Puranik, A. K. Patra, P. U. Sastry, P. Dastidar, *Soft Matter* **2011**, 7, 3634–3641.
- [36] P. Sahoo, R. Sankolli, H.-Y. Lee, S. R. Raghavan, P. Dastidar, *Chem. Eur. J.* **2012**, 18, 8057–8063.
- [37] J. Majumder, J. Deb, M. R. Das, S. S. Jana, P. Dastidar, *Chem. Commun.* **2014**, 50, 1671–1674.
- [38] a) M. Suzuki, K. Hanabusa, *Chem. Soc. Rev.* **2009**, 38, 967–975; b) X. Yan, P. Zhua, J. Li, *Chem. Soc. Rev.* **2010**, 39, 1877–1890.
- [39] S. A. Khan, J. R. Royer, S. R. Raghavan, *Aviation Fuels with Improved Fire Safety: A Proceedings* **1997**, 6, 31–46.
- [40] P. Martinetto, P. Terech, A. Grand, R. Ramasscul, E. Dooryhe, M. Anne, *J. Phys. Chem. A* **2006**, 110, 15127–15133.
- [41] E. Ostuni, P. Kamaras, R. G. Weiss, *Angew. Chem. Int. Ed. Engl.* **1996**, 35, 1324–1326; *Angew. Chem.* **1996**, 108, 1423–1425.

Received: February 13, 2014

Revised: April 18, 2014

Published online: ■ ■ ■, 0000

# FULL PAPER

**Healing is a matter of time:** A series of bis-amides derived from L-phenylalanine and L-alanine displayed moderate to good gelation ability with various solvents. Structure–property correlation using single-crystal and powder X-ray diffraction on selected gels was attempted. One of the gelator resulted in a gel with outstanding load-bearing and self-healing properties. The 1,2-dichlorobenzene gel of this gelator was so strong that letters could be carved into a thin slice of the gel.



## Supramolecular Gels

Uttam Kumar Das,  
Subhabrata Banerjee,  
Parthasarathi Dastidar\* — ■■■■—■■■■

**Remarkable Shape-Sustaining, Load-Bearing, and Self-Healing Properties Displayed by a Supramolecular Gel Derived from a Bis-pyridyl-bis-amide of L-Phenyl Alanine**

